

MODELING AND ANALYSIS OF 3D FREE VIBRATIONS OF THERMOELASTIC ECCENTRIC HOLLOW CYLINDER

HARJIT SINGH

Abstract: The aim of the paper is to study the wave propagation in a simply supported homogeneous isotropic, thermally conducting eccentric circular cylinder in context of three-dimensional linear coupled thermo elasticity. The displacement potential functions have been introduced to decouple purely shear and longitudinal motions. The surfaces of the cylinder are subjected to stress free and thermally insulated or isothermal boundary conditions. A combination of modified Bessel function and translation addition theorem for cylindrical wave functions has been employed to develop the exact solution. The computed lowest frequency and dissipation factor versus truncation constant is studied and are plotted in the form of dispersion curves with the support of MATLAB. The numerical solution of secular relation has been obtained to compute lowest frequency versus dimensionless eccentricities for different geometrical parameters of eccentric hollow cylinder. The computer simulated results have been obtained with the help of MATLAB software programming and are presented graphically.

Keywords: Thermo elasticity, Bessel Function, Mathematical Modeling, MATLAB.

Introduction: Hutchinson and El-Azhari [1] studied the vibrational analysis of hollow cylinder by using a Bessel series solution. Soldatos and Hadhgeorgion [2] used an iterative method to study the three-dimensional vibrations in elastic cylindrical shells and panels. Mofakami et al. [3] studied the free vibrations of hollow finite cylinder by using the separation of variable technique. Mirsky [4] examined wave propagation in a transversely isotropic elastic circular cylinder. Martin and Berger [5] studied the wave propagation in pyroelectric cylinder of arbitrary shape. Sharma [6] studied the wave propagation in simply supported, homogeneous transversely isotropic coupled thermo elastic cylindrical panel. Sharma and Sharma [7] extended the analysis [6] to study the vibrations of transversely isotropic thermoelastic cylindrical panel in the context of generalized thermoelasticity. Khurashia and Rewtant [8] investigated the effect of presence of eccentric hole on free vibration of a thin circular plate. Laura et al. [9] used Rayleigh Ritz and finite element methods to determine the effect of circumferential variations in wall thickness on eigenfrequencies and axisymmetric modes of a nonuniform ring. Yu and Zhong [10] investigated the flexural free vibrations of moderately thick eccentric annular plate. Hasheminejad and Mirzaei [11] studied the free vibration analysis of an eccentric elastic hollow cylinder by using the translation addition theorem for cylindrical wave functions. The present paper is devoted to investigate the three-dimensional free vibrations in a simply supported homogeneous isotropic thermoelastic

finite circular cylinder with an eccentrically located inner circular cavity.

2. Mathematical model: Consider a homogeneous isotropic, thermally conducting, elastic hollow cylinder in the undisturbed state and at uniform temperature T_0 initially. Upon employing model of linear coupled thermoelasticity, the constitutive equation may be written as

$$\sigma_{ij} = \lambda e_{kk} \delta_{ij} + 2\mu e_{ij} - \beta T \delta_{ij}, \quad i, j = 1, 2, 3 \quad (1)$$

where $T(r, \theta, z, t)$ is the temperature change; δ_{ij} is Kronecker delta symbol; λ, μ are Lamé's parameters, $\beta = (3\lambda + 2\mu)\alpha_T$ is coupling parameter of thermal and mechanical fields, α_T is the coefficients of linear thermal expansion.

The governing field equations of motion and heat conduction for such materials, in the absence of body force and heat source, are given by

$$\rho \ddot{\bar{u}} = \mu \nabla^2 \bar{u} + (\lambda + \mu) \nabla (\nabla \cdot \bar{u}) - \beta \nabla T \quad (2)$$

$$K \nabla^2 T - \rho C_e \dot{T} = \beta T_0 (\nabla \cdot \dot{\bar{u}}) \quad (3)$$

$$\text{where } \nabla^2 = \frac{\partial^2}{\partial r^2} + \frac{1}{r} \frac{\partial}{\partial r} + \frac{1}{r^2} \frac{\partial^2}{\partial \theta^2} + \frac{\partial^2}{\partial z^2}$$

$$\text{and } \bar{u}(r, \theta, z, t) = (u_r, u_\theta, u_z)$$

are the displacement vectors; α_T and K are respectively, the coefficients of linear thermal expansion and thermal conductivity; ρ and C_e are the mass density and specific heat at constant strain, respectively.

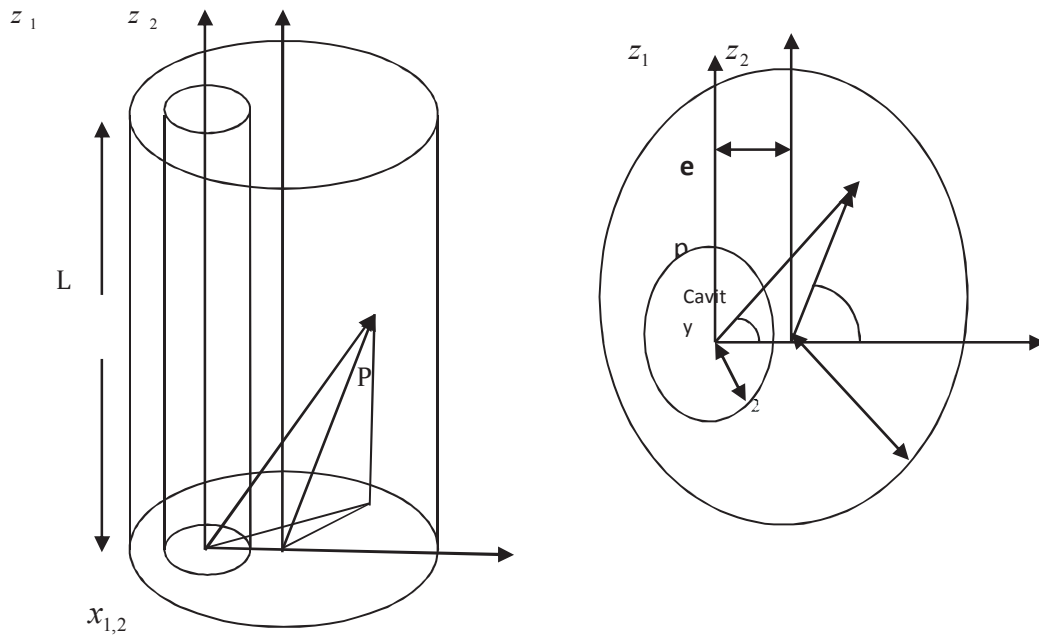


Fig. 1. Geometry of Problem

In order to simplify the equations (1)-(3), we define the following non-dimensional quantities

$$r' = \frac{\omega^*}{c_1} r, z' = \frac{\omega^*}{c_1} z, t' = \omega^* t \quad u'_i = \frac{\rho c_1 \omega^*}{\beta T_0} u_i,$$

$$T' = \frac{T}{T_0}, \sigma'_{ij} = \frac{\sigma_{ij}}{\beta T_0}, \quad e'_{ij} = \frac{\rho c_1^2}{\beta T_0} e_{ij}, \quad \omega' = \frac{\omega}{\omega^*},$$

$$\omega^* = \frac{C_e(\lambda + 2\mu)}{K}, \quad \varepsilon_T = \frac{\beta^2 T_0}{\rho C_e(\lambda + 2\mu)}, \quad \delta^2 = \frac{c_2^2}{c_1^2},$$

$$c_1^2 = \frac{\lambda + 2\mu}{\rho}, \quad c_2^2 = \frac{\mu}{\rho}, \quad a' = \frac{\omega^*}{c_1} a, \quad b' = \frac{\omega^*}{c_1} b$$

(4)

Here ε_T is the thermoelastic coupling parameter, c_1 , c_2 are respectively velocities of longitudinal and transverse fields.

Introducing quantities defined by (4) in equations (1), (2) and (3) we obtain (on suppressing the primes for convenience)

$$\ddot{\vec{u}} = \delta^2 \nabla^2 \vec{u} + (1 - \delta^2) \nabla(\nabla \cdot \vec{u}) - \nabla T \quad (5)$$

$$\nabla^2 T - \dot{T} = \varepsilon_T (\nabla \cdot \dot{\vec{u}}) \quad (6)$$

$$\sigma_{ij} = (1 - 2\delta^2) e_{kk} \delta_{ij} + 2\delta^2 e_{ij} - T \delta_{ij} \quad (7)$$

In order to facilitate the analysis we introduce scalar potential function ϕ and vector potential function $\vec{\psi}$ with the Helmholtz decomposition theorem through the relation given below

$$\vec{u} = \nabla \phi + \nabla \times \vec{\psi}, \quad \nabla \cdot \vec{\psi} = 0 \quad (8)$$

The above decomposition provide us to separate the equation of motion (5) and heat conduction (6) as

$$\nabla^2 \phi - T = \ddot{\phi} \quad (9)$$

$$\delta^2 \nabla^2 \vec{\psi} = \ddot{\vec{\psi}} \quad (10)$$

$$\nabla^2 T - \dot{T} = \varepsilon_T \nabla^2 \dot{\phi} \quad (11)$$

On the account of the condition of zero divergence $\nabla \cdot \vec{\psi} = 0$, only two of three components of $\vec{\psi}$ are independent. Accordingly, the above system (9)-(11) are reduced to the scalar wave equations

$$\nabla^2 \phi - T = \ddot{\phi} \quad (12)$$

$$\delta^2 \nabla^2 \psi = \ddot{\psi} \quad (13)$$

$$\delta^2 \nabla^2 \chi = \ddot{\chi} \quad (14)$$

$$\nabla^2 T - \dot{T} = \varepsilon_T \nabla^2 \dot{\phi} \quad (15)$$

3. Solution of the problem

We consider the free vibrations of a hollow cylinder which is subjected to the traction free and thermally insulated boundary conditions with simply supported edge. We can write

$$\phi(r, \theta, z, t) = \sum_{m=-\infty}^{\infty} \sum_{n=-\infty}^{\infty} \bar{\phi}(r) \sin(\gamma_m z) \exp\{i(n\theta - \omega t)\}$$

$$T(r, \theta, z, t) = \sum_{m=-\infty}^{\infty} \sum_{n=-\infty}^{\infty} \bar{T}(r) \sin(\gamma_m z) \exp\{i(n\theta - \omega t)\}$$

$$\psi(r, \theta, z, t) = \sum_{m=-\infty}^{\infty} \sum_{n=-\infty}^{\infty} \bar{\psi}(r) \sin(\gamma_m z) \exp\{i(n\theta - \omega t)\}$$

$$\chi(r, \theta, z, t) = \sum_{m=-\infty}^{\infty} \sum_{n=-\infty}^{\infty} \bar{\chi}(r) \cos(\gamma_m z) \exp\{i(n\theta - \omega t)\}$$

(16)

On using solution (16) in equations (12)-(15), we obtain

$$(\nabla_2^2 + \tau^2)\bar{\phi} - \bar{T} = 0 \tag{17.1}$$

$$i\omega\varepsilon_T(\nabla_2^2 - \gamma_m^2)\bar{\phi} + (\nabla_2^2 + \eta^2)\bar{T} = 0 \tag{17.2}$$

$$(\nabla_2^2 + \alpha^2)\bar{\psi} = 0 \tag{17.3}$$

$$(\nabla_2^2 + \alpha^2)\bar{\chi} = 0 \tag{17.4}$$

$$\text{where } \nabla_2^2 = \frac{\partial^2}{\partial r^2} + \frac{1}{r} \frac{\partial}{\partial r} - \frac{n^2}{r^2}$$

$$\gamma_m = \frac{m\pi}{L}, \tau^2 = \omega^2 - \gamma_m^2,$$

$$\alpha^2 = \frac{\omega^2}{\delta^2} - \gamma_m^2, \eta^2 = i\omega - \gamma_m^2 \tag{18}$$

The equations (17.3) and (17.4) being Bessel's equations have possible solutions as

$$\bar{\psi}(r) = \begin{cases} c_{nm}J_n(\alpha r) + d_{nm}Y_n(\alpha r) & , \alpha^2 > 0 \\ c_{nm}r^n + d_{nm}r^{-n} & , \alpha^2 = 0 \\ c_{nm}I_n(\alpha' r) + d_{nm}K_n(\alpha' r) & , \alpha^2 < 0 \end{cases}$$

$$\bar{\chi}(r) = \begin{cases} e_{nm}J_n(\alpha r) + f_{nm}Y_n(\alpha r) & , \alpha^2 > 0 \\ e_{nm}r^n + f_{nm}r^{-n} & , \alpha^2 = 0 \\ e_{nm}I_n(\alpha' r) + f_{nm}K_n(\alpha' r) & , \alpha^2 < 0 \end{cases} \tag{19}$$

where $\alpha'^2 = -\alpha^2$. Here J_n and Y_n (I_n and K_n) are respectively the Bessel functions (modified Bessel functions) of the first and second kind; c_{nm}, d_{nm}, e_{nm} and f_{nm} are arbitrary constants to be determined. Generally, $\alpha^2 \neq 0$, so the specific situation $\alpha^2 = 0$ will not be discussed in the following analysis.

From the equations (17.1) and (17.2), we obtain

$$(\nabla_2^2 + m_1^2)(\nabla_2^2 + m_2^2)\bar{H} = 0 \tag{20}$$

where \bar{H} may be any one of the function $\bar{\phi}$ or \bar{T} and the quantities m_i^2 ($i = 1, 2$) are the roots of complex algebraic equation

$$m^4 + Am^2 + B = 0 \tag{21}$$

where $A = \tau^2 + \eta^2 + i\omega\varepsilon_T$ $B = \tau^2\eta^2 - i\omega\varepsilon_T\gamma_m^2$

Upon solving the equations (21) and noting that the roots m_i^2 ($i = 1, 2$) are complex, the functions $\bar{\phi}$ and \bar{T} being solution of equations (17.1) and (17.2) are obtained as

$$\bar{\phi}(r) = \sum_{i=1}^2 [a_{nm}^{[i]}J_n(m_i r) + b_{nm}^{[i]}Y_n(m_i r)] \tag{22}$$

$$\bar{T}(r) = \sum_{i=1}^2 L_i [a_{nm}^{[i]}J_n(m_i r) + b_{nm}^{[i]}Y_n(m_i r)] \tag{23}$$

where $L_i = \tau^2 - m_i^2$, ($i = 1, 2$)

In the following analysis, we proceed with our derivation by taking $\alpha^2 > 0$ (the derivation for $\alpha^2 < 0$ is obviously similar) in equation (19) so that the solution of (17.3) and (17.4) is written as

$$\bar{\psi}(r) = c_{nm}J_n(\alpha r) + d_{nm}Y_n(\alpha r) \tag{24}$$

$$\bar{\chi}(r) = e_{nm}J_n(\alpha r) + f_{nm}Y_n(\alpha r) \tag{25}$$

Thus the displacement potential and temperature change in equation (18) becomes

$$\phi(r, \theta, z, t) = \sum_{m=-\infty}^{\infty} \sum_{n=-\infty}^{\infty} \sum_{i=1}^2 [a_{nm}^{[i]}J_n(m_i r) + b_{nm}^{[i]}Y_n(m_i r)] \sin(\gamma_m z) \exp\{i(n\theta - \omega t)\}$$

$$T(r, \theta, z, t) = \sum_{m=-\infty}^{\infty} \sum_{n=-\infty}^{\infty} \sum_{i=1}^2 L_i [a_{nm}^{[i]}J_n(m_i r) + b_{nm}^{[i]}Y_n(m_i r)] \sin(\gamma_m z) \exp\{i(n\theta - \omega t)\}$$

$$\psi(r, \theta, z, t) = \sum_{m=-\infty}^{\infty} \sum_{n=-\infty}^{\infty} [c_{nm}J_n(\alpha r) + d_{nm}Y_n(\alpha r)] \sin(\gamma_m z) \exp\{i(n\theta - \omega t)\}$$

$$\chi(r, \theta, z, t) = \sum_{m=-\infty}^{\infty} \sum_{n=-\infty}^{\infty} [e_{nm}J_n(\alpha r) + f_{nm}Y_n(\alpha r)] \cos(\gamma_m z) \exp\{i(n\theta - \omega t)\} \tag{26}$$

4. Field expansions: The geometry of the problem is depicted in Fig. 1. Two cylindrical systems (r_1, θ_1, z_1) and (r_2, θ_2, z_2) are introduced to describe the field within the circle. The axes of the cylinder are parallel, and $z_1 = z_2 = z$. The origin to origin separation is e ($e_{\max} = b - a$) and point P is an arbitrary field point within the eccentric cylinder, outside the cylindrical cavity. Upon using equation (28), the field expansions for longitudinal, shear waves and temperature change within the eccentric cylinder with respect to the (r_1, θ_1, z) coordinate system may be written as

$$\phi(r_1, \theta_1, z, \omega) = \sum_{m=-\infty}^{\infty} \sum_{n=-\infty}^{\infty} \sum_{i=1}^2 [a_{nm}^{[i]}J_n(m_i r_1) + b_{nm}^{[i]}Y_n(m_i r_1)] \sin(\gamma_m z) \exp\{in\theta_1\}$$

$$T(r_1, \theta_1, z, \omega) = \sum_{m=-\infty}^{\infty} \sum_{n=-\infty}^{\infty} \sum_{i=1}^2 L_i [a_{nm}^{[i]}J_n(m_i r_1) + b_{nm}^{[i]}Y_n(m_i r_1)] \sin(\gamma_m z) \exp\{in\theta_1\}$$

$$\psi(r_1, \theta_1, z, \omega) = \sum_{m=-\infty}^{\infty} \sum_{n=-\infty}^{\infty} [c_{nm}J_n(\alpha r_1) + d_{nm}Y_n(\alpha r_1)] \sin(\gamma_m z) \exp\{in\theta_1\}$$

$$\chi(r_1, \theta_1, z, \omega) = \sum_{m=-\infty}^{\infty} \sum_{n=-\infty}^{\infty} [e_{nm}J_n(\alpha r_1) + f_{nm}Y_n(\alpha r_1)] \cos(\gamma_m z) \exp\{in\theta_1\} \tag{27}$$

where (m_i, α, γ) are separation constants.

5. Displacements and Stresses: The displacement components in cylindrical coordinates in terms of compressional and shear wave potentials may simply be written as [12]

$$\begin{aligned}
 u_r &= \frac{\partial \phi}{\partial r} + \frac{1}{r} \frac{\partial \psi}{\partial \theta} + \frac{\partial^2 \chi}{\partial r \partial z} \\
 u_\theta &= \frac{1}{r} \frac{\partial \phi}{\partial \theta} - \frac{\partial \psi}{\partial r} + \frac{1}{r} \frac{\partial^2 \chi}{\partial \theta \partial z} \\
 u_z &= \frac{\partial \phi}{\partial z} - \left[\frac{1}{r} \frac{\partial}{\partial r} \left(r \frac{\partial \chi}{\partial r} \right) + \frac{1}{r^2} \frac{\partial^2 \chi}{\partial \theta^2} \right] \quad (28)
 \end{aligned}$$

Further, the relevant stress components are given by

$$\begin{aligned}
 \sigma_{rr} &= \delta^2 \left[\frac{\partial^2 \phi}{\partial r^2} + \frac{\partial}{\partial r} \left(\frac{1}{r} \frac{\partial \psi}{\partial \theta} \right) + \frac{\partial^3 \chi}{\partial r^2 \partial z} \right] + \omega^2 (\delta^2 - 1) \phi - \delta^2 T \\
 \sigma_{r\theta} &= \delta^2 \left[2 \frac{\partial}{\partial r} \left(\frac{1}{r} \frac{\partial \phi}{\partial \theta} \right) + \left[\frac{1}{r^2} \frac{\partial^2 \psi}{\partial \theta^2} - r \frac{\partial}{\partial r} \left(\frac{1}{r} \frac{\partial \psi}{\partial r} \right) + 2 \frac{\partial}{\partial r} \left(\frac{1}{r} \frac{\partial^2 \chi}{\partial z \partial \theta} \right) \right] \right] \\
 \sigma_{rz} &= \delta^2 \left[2 \frac{\partial^2 \phi}{\partial r \partial z} + \frac{1}{r} \frac{\partial^2 \psi}{\partial \theta \partial z} + 2 \frac{\partial^3 \chi}{\partial z^2 \partial r} - \frac{\partial}{\partial r} (\nabla^2 \chi) \right] \quad (29)
 \end{aligned}$$

Direct substitution of field expansions (27) into the field equations (28) and (29), leads to

$$\begin{aligned}
 u_r(r_1, \theta_1, z, \omega) &= \sum_{m=-\infty}^{\infty} \sum_{n=-\infty}^{\infty} \left[\begin{aligned} &a_{nm}^{[1]} P_{1n}^{[1]} + b_{nm}^{[1]} P_{1n}^{[2]} \\ &+ a_{nm}^{[2]} P_{2n}^{[1]} + b_{nm}^{[2]} P_{2n}^{[2]} \\ &+ c_{nm}^{[1]} P_{3n}^{[1]} + d_{nm}^{[1]} P_{3n}^{[2]} \\ &+ e_{nm}^{[1]} P_{4n}^{[1]} + f_{nm}^{[1]} P_{4n}^{[2]} \end{aligned} \right] \sin(\gamma_m z) \exp(in\theta_1) \\
 u_\theta(r_1, \theta_1, z, \omega) &= \sum_{m=-\infty}^{\infty} \sum_{n=-\infty}^{\infty} \left[\begin{aligned} &a_{nm}^{[1]} P_{5n}^{[1]} + b_{nm}^{[1]} P_{5n}^{[2]} \\ &+ a_{nm}^{[2]} P_{6n}^{[1]} + b_{nm}^{[2]} P_{6n}^{[2]} \\ &+ c_{nm}^{[1]} P_{7n}^{[1]} + d_{nm}^{[1]} P_{7n}^{[2]} \\ &+ e_{nm}^{[1]} P_{8n}^{[1]} + f_{nm}^{[1]} P_{8n}^{[2]} \end{aligned} \right] \sin(\gamma_m z) \exp(in\theta_1) \\
 u_z(r_1, \theta_1, z, \omega) &= \sum_{m=-\infty}^{\infty} \sum_{n=-\infty}^{\infty} \left[\begin{aligned} &a_{nm}^{[1]} P_{9n}^{[1]} + b_{nm}^{[1]} P_{9n}^{[2]} \\ &+ a_{nm}^{[2]} P_{10n}^{[1]} + b_{nm}^{[2]} P_{10n}^{[2]} \\ &+ c_{nm}^{[1]} P_{11n}^{[1]} + d_{nm}^{[1]} P_{11n}^{[2]} \\ &+ e_{nm}^{[1]} P_{12n}^{[1]} + f_{nm}^{[1]} P_{12n}^{[2]} \end{aligned} \right] \cos(\gamma_m z) \exp(in\theta_1) \quad (30)
 \end{aligned}$$

$$\begin{aligned}
 \sigma_{rr}(r_1, \theta_1, z, \omega) &= \sum_{m=-\infty}^{\infty} \sum_{n=-\infty}^{\infty} \left[\begin{aligned} &a_{nm}^{[1]} Q_{1n}^{[1]} + b_{nm}^{[1]} Q_{1n}^{[2]} \\ &+ a_{nm}^{[2]} Q_{2n}^{[1]} + b_{nm}^{[2]} Q_{2n}^{[2]} \\ &+ c_{nm}^{[1]} Q_{3n}^{[1]} + d_{nm}^{[1]} Q_{3n}^{[2]} \\ &+ e_{nm}^{[1]} Q_{4n}^{[1]} + f_{nm}^{[1]} Q_{4n}^{[2]} \end{aligned} \right] \sin(\gamma_m z) \exp(in\theta_1) \\
 \sigma_{r\theta}(r_1, \theta_1, z, \omega) &= \sum_{m=-\infty}^{\infty} \sum_{n=-\infty}^{\infty} \left[\begin{aligned} &a_{nm}^{[1]} Q_{5n}^{[1]} + b_{nm}^{[1]} Q_{5n}^{[2]} \\ &+ a_{nm}^{[2]} Q_{6n}^{[1]} + b_{nm}^{[2]} Q_{6n}^{[2]} \\ &+ c_{nm}^{[1]} Q_{7n}^{[1]} + d_{nm}^{[1]} Q_{7n}^{[2]} \\ &+ e_{nm}^{[1]} Q_{8n}^{[1]} + f_{nm}^{[1]} Q_{8n}^{[2]} \end{aligned} \right] \sin(\gamma_m z) \exp(in\theta_1) \\
 \sigma_{rz}(r_1, \theta_1, z, \omega) &= \sum_{m=-\infty}^{\infty} \sum_{n=-\infty}^{\infty} \left[\begin{aligned} &a_{nm}^{[1]} Q_{9n}^{[1]} + b_{nm}^{[1]} Q_{9n}^{[2]} \\ &+ a_{nm}^{[2]} Q_{10n}^{[1]} + b_{nm}^{[2]} Q_{10n}^{[2]} \\ &+ c_{nm}^{[1]} Q_{11n}^{[1]} + d_{nm}^{[1]} Q_{11n}^{[2]} \\ &+ e_{nm}^{[1]} Q_{12n}^{[1]} + f_{nm}^{[1]} Q_{12n}^{[2]} \end{aligned} \right] \cos(\gamma_m z) \exp(in\theta_1)
 \end{aligned}$$

where the expressions for $P_{in}^{[s]}(r_j, \gamma_m, \omega)$ and $Q_{in}^{[s]}(r_j, \gamma_m, \omega)$ ($i = 1, 2, \dots, 12$; $j, s = 1, 2$) are

given in the Appendix

6. Boundary conditions: (a) *Mechanical condition*

The inner/outer surfaces are assumed to be traction

$$\begin{aligned}
 \sigma_{rr}(r_1 = a; \theta_1; z = 0, L; \omega) &= 0 \\
 \sigma_{r\theta}(r_1 = a; \theta_1; z = 0, L; \omega) &= 0 \quad (32) \\
 \sigma_{rz}(r_1 = a; \theta_1; z = 0, L; \omega) &= 0
 \end{aligned}$$

$$\begin{aligned}
 \sigma_{rr}(r_2 = b; \theta_2; z = 0, L; \omega) &= 0 \\
 \sigma_{r\theta}(r_2 = b; \theta_2; z = 0, L; \omega) &= 0 \quad (33) \\
 \sigma_{rz}(r_2 = b; \theta_2; z = 0, L; \omega) &= 0
 \end{aligned}$$

(b) *Thermal condition*

The inner/outer surfaces are assumed to be thermally insulated which leads to

$$\begin{aligned}
 T_r(r_1 = a; \theta_1; z = 0, L; \omega) &= 0 \quad (34) \\
 T_r(r_2 = b; \theta_2; z = 0, L; \omega) &= 0 \quad (35)
 \end{aligned}$$

7. Frequency equation: Using (31), enforcement to inner surface and thermal boundary conditions (32) and (34) lead to the following equations

$$\begin{aligned}
 &a_{nm}^{[1]} Q_{1n}^{[1]}(a, \gamma_m, \omega) + b_{nm}^{[1]} Q_{1n}^{[2]}(a, \gamma_m, \omega) \\
 &+ a_{nm}^{[2]} Q_{2n}^{[1]}(a, \gamma_m, \omega) + b_{nm}^{[2]} Q_{2n}^{[2]}(a, \gamma_m, \omega) \\
 &+ c_{nm}^{[1]} Q_{3n}^{[1]}(a, \gamma_m, \omega) + d_{nm}^{[1]} Q_{3n}^{[2]}(a, \gamma_m, \omega) \\
 &+ e_{nm}^{[1]} Q_{4n}^{[1]}(a, \gamma_m, \omega) + f_{nm}^{[1]} Q_{4n}^{[2]}(a, \gamma_m, \omega) = 0 \\
 &a_{nm}^{[1]} Q_{5n}^{[1]}(a, \gamma_m, \omega) + b_{nm}^{[1]} Q_{5n}^{[2]}(a, \gamma_m, \omega) \\
 &+ a_{nm}^{[2]} Q_{6n}^{[1]}(a, \gamma_m, \omega) + b_{nm}^{[2]} Q_{6n}^{[2]}(a, \gamma_m, \omega) \\
 &+ c_{nm}^{[1]} Q_{7n}^{[1]}(a, \gamma_m, \omega) + d_{nm}^{[1]} Q_{7n}^{[2]}(a, \gamma_m, \omega) \\
 &+ e_{nm}^{[1]} Q_{8n}^{[1]}(a, \gamma_m, \omega) + f_{nm}^{[1]} Q_{8n}^{[2]}(a, \gamma_m, \omega) = 0 \\
 &a_{nm}^{[1]} Q_{9n}^{[1]}(a, \gamma_m, \omega) + b_{nm}^{[1]} Q_{9n}^{[2]}(a, \gamma_m, \omega) \\
 &+ a_{nm}^{[2]} Q_{10n}^{[1]}(a, \gamma_m, \omega) + b_{nm}^{[2]} Q_{10n}^{[2]}(a, \gamma_m, \omega) \\
 &+ c_{nm}^{[1]} Q_{11n}^{[1]}(a, \gamma_m, \omega) + d_{nm}^{[1]} Q_{11n}^{[2]}(a, \gamma_m, \omega) \\
 &+ e_{nm}^{[1]} Q_{12n}^{[1]}(a, \gamma_m, \omega) + f_{nm}^{[1]} Q_{12n}^{[2]}(a, \gamma_m, \omega) = 0 \\
 &a_{nm}^{[1]} Q_{13n}^{[1]}(a, \gamma_m, \omega) + b_{nm}^{[1]} Q_{13n}^{[2]}(a, \gamma_m, \omega) \\
 &+ a_{nm}^{[2]} Q_{14n}^{[1]}(a, \gamma_m, \omega) + b_{nm}^{[2]} Q_{14n}^{[2]}(a, \gamma_m, \omega) \\
 &+ c_{nm}^{[1]} Q_{15n}^{[1]}(a, \gamma_m, \omega) + d_{nm}^{[1]} Q_{15n}^{[2]}(a, \gamma_m, \omega) \\
 &+ e_{nm}^{[1]} Q_{16n}^{[1]}(a, \gamma_m, \omega) + f_{nm}^{[1]} Q_{16n}^{[2]}(a, \gamma_m, \omega) = 0 \quad (36)
 \end{aligned}$$

where $n, m = \dots, -2, -1, 0, 1, 2, \dots$. Satisfaction of the outer boundary condition is far more complicated, and will be achieved next by application

of translation addition theorem for cylindrical wave functions.

8. Translation addition theorem: The cylindrical wave function of inner coordinate system (r_1, θ_1, z_1) in terms of cylindrical wave functions of outer coordinate system (r_2, θ_2, z_2) by application of translation addition theorem for cylindrical wave functions [13]:

$$\begin{Bmatrix} J_n(\kappa r_1) \\ Y_n(\kappa r_1) \end{Bmatrix} e^{in\theta_1} = \sum_{k=-\infty}^{\infty} J_{n-k}(\kappa e) \begin{Bmatrix} J_k(\kappa r_2) \\ Y_k(\kappa r_2) \end{Bmatrix} e^{ik\theta_2} \quad (37)$$

where $e < r_2 (0 \leq r_2 \leq b)$, and noting $e_{\max} = b - a$, when later imposing boundary conditions at $r_2 = b$, the condition $e < r_2 = b$, will be clearly satisfied. Using above expression in (29) in order to express field potential with respect to second coordinate system (r_2, θ_2, z) i.e.

$$\begin{aligned} \phi(r_2, \theta_2, z, \omega) &= \sum_{m=-\infty}^{\infty} \sum_{n=-\infty}^{\infty} \sum_{i=1}^2 [A_{nm}^{[i]} J_n(m_i r_2) + B_{nm}^{[i]} Y_n(m_i r_2)] \sin(\gamma_m z) \exp\{in\theta_2\} \\ T(r_2, \theta_2, z, \omega) &= \sum_{m=-\infty}^{\infty} \sum_{n=-\infty}^{\infty} \sum_{i=1}^2 L_i [A_{nm}^{[i]} J_n(m_i r_2) + B_{nm}^{[i]} Y_n(m_i r_2)] \sin(\gamma_m z) \exp\{in\theta_2\} \\ \psi(r_2, \theta_2, z, \omega) &= \sum_{m=-\infty}^{\infty} \sum_{n=-\infty}^{\infty} [C_{nm} J_n(\alpha r_2) + D_{nm} Y_n(\alpha r_2)] \sin(\gamma_m z) \exp\{in\theta_2\} \\ \chi(r_2, \theta_2, z, \omega) &= \sum_{m=-\infty}^{\infty} \sum_{n=-\infty}^{\infty} [E_{nm} J_n(\alpha r_2) + F_{nm} Y_n(\alpha r_2)] \cos(\gamma_m z) \exp\{in\theta_2\} \end{aligned} \quad (38)$$

where

$$\begin{aligned} A_{nm}^{[i]} &= \sum_{k=-\infty}^{\infty} a_{km}^{[i]} J_{k-n}(m_i e), \quad B_{nm}^{[i]} = \sum_{k=-\infty}^{\infty} b_{km}^{[i]} J_{k-n}(m_i e), \quad i = 1, 2 \\ C_{nm} &= \sum_{k=-\infty}^{\infty} c_{km} J_{k-n}(\alpha e), \quad D_{nm} = \sum_{k=-\infty}^{\infty} d_{km} J_{k-n}(\alpha e) \\ E_{nm} &= \sum_{k=-\infty}^{\infty} e_{km} J_{k-n}(\alpha e), \quad F_{nm} = \sum_{k=-\infty}^{\infty} f_{km} J_{k-n}(\alpha e) \end{aligned} \quad (39)$$

and the index "k" has been interchanged with index "n" for convenience. Direct substitution of field expansions (38) into field equations (29), leads to

$$\begin{aligned} \sigma_{rr}(r_2, \theta_2, z, \omega) &= \sum_{m=-\infty}^{\infty} \sum_{n=-\infty}^{\infty} \begin{bmatrix} A_{nm}^{[1]} Q_n^{[1]} + B_{nm}^{[1]} Q_n^{[2]} \\ + A_{nm}^{[2]} Q_n^{[1]} + B_{nm}^{[2]} Q_n^{[2]} \\ + C_{nm} Q_{3n}^{[1]} + D_{nm} Q_{3n}^{[2]} \\ + E_{nm} Q_{4n}^{[1]} + F_{nm} Q_{4n}^{[2]} \end{bmatrix} \sin(\gamma_m z) \exp\{in\theta_2\} \\ \sigma_{r\theta}(r_2, \theta_2, z, \omega) &= \sum_{m=-\infty}^{\infty} \sum_{n=-\infty}^{\infty} \begin{bmatrix} A_{nm}^{[1]} Q_n^{[1]} + B_{nm}^{[1]} Q_n^{[2]} \\ + A_{nm}^{[2]} Q_n^{[1]} + B_{nm}^{[2]} Q_n^{[2]} \\ + C_{nm} Q_{7n}^{[1]} + D_{nm} Q_{7n}^{[2]} \\ + E_{nm} Q_{8n}^{[1]} + F_{nm} Q_{8n}^{[2]} \end{bmatrix} \sin(\gamma_m z) \exp\{in\theta_2\} \\ \sigma_{rz}(r_2, \theta_2, z, \omega) &= \sum_{m=-\infty}^{\infty} \sum_{n=-\infty}^{\infty} \begin{bmatrix} A_{nm}^{[1]} Q_n^{[1]} + B_{nm}^{[1]} Q_n^{[2]} \\ + A_{nm}^{[2]} Q_n^{[1]} + B_{nm}^{[2]} Q_n^{[2]} \\ + C_{nm} Q_{1n}^{[1]} + D_{nm} Q_{1n}^{[2]} \\ + E_{nm} Q_{12n}^{[1]} + F_{nm} Q_{12n}^{[2]} \end{bmatrix} \cos(\gamma_m z) \exp\{in\theta_2\} \end{aligned} \quad (40)$$

Imposing outer surface condition (33) and (35), while keeping in mind the orthogonality of transcendental functions, leads to the following equations

$$\begin{aligned} &A_{nm}^{[1]} Q_{1n}^{[1]}(b, \gamma_m, \omega) + B_{nm}^{[1]} Q_{1n}^{[2]}(b, \gamma_m, \omega) \\ &+ A_{nm}^{[2]} Q_{2n}^{[1]}(b, \gamma_m, \omega) + B_{nm}^{[2]} Q_{2n}^{[2]}(b, \gamma_m, \omega) \\ &+ C_{nm} Q_{3n}^{[1]}(b, \gamma_m, \omega) + D_{nm} Q_{3n}^{[2]}(b, \gamma_m, \omega) \\ &+ E_{nm} Q_{4n}^{[1]}(b, \gamma_m, \omega) + F_{nm} Q_{4n}^{[2]}(b, \gamma_m, \omega) = 0 \\ &A_{nm}^{[1]} Q_{5n}^{[1]}(b, \gamma_m, \omega) + B_{nm}^{[1]} Q_{5n}^{[2]}(b, \gamma_m, \omega) \\ &+ A_{nm}^{[2]} Q_{6n}^{[1]}(b, \gamma_m, \omega) + B_{nm}^{[2]} Q_{6n}^{[2]}(b, \gamma_m, \omega) \\ &+ C_{nm} Q_{7n}^{[1]}(b, \gamma_m, \omega) + D_{nm} Q_{7n}^{[2]}(b, \gamma_m, \omega) \\ &+ E_{nm} Q_{8n}^{[1]}(b, \gamma_m, \omega) + F_{nm} Q_{8n}^{[2]}(b, \gamma_m, \omega) = 0 \\ &A_{nm}^{[1]} Q_{9n}^{[1]}(b, \gamma_m, \omega) + B_{nm}^{[1]} Q_{9n}^{[2]}(b, \gamma_m, \omega) \\ &+ A_{nm}^{[2]} Q_{10n}^{[1]}(b, \gamma_m, \omega) + B_{nm}^{[2]} Q_{10n}^{[2]}(b, \gamma_m, \omega) \\ &+ C_{nm} Q_{11n}^{[1]}(b, \gamma_m, \omega) + D_{nm} Q_{11n}^{[2]}(b, \gamma_m, \omega) \\ &+ E_{nm} Q_{12n}^{[1]}(b, \gamma_m, \omega) + F_{nm} Q_{12n}^{[2]}(b, \gamma_m, \omega) = 0 \\ &A_{nm}^{[1]} Q_{13n}^{[1]}(b, \gamma_m, \omega) + B_{nm}^{[1]} Q_{13n}^{[2]}(b, \gamma_m, \omega) \\ &+ A_{nm}^{[2]} Q_{14n}^{[1]}(b, \gamma_m, \omega) + B_{nm}^{[2]} Q_{14n}^{[2]}(b, \gamma_m, \omega) \\ &+ C_{nm} Q_{15n}^{[1]}(b, \gamma_m, \omega) + D_{nm} Q_{15n}^{[2]}(b, \gamma_m, \omega) \\ &+ E_{nm} Q_{16n}^{[1]}(b, \gamma_m, \omega) + F_{nm} Q_{16n}^{[2]}(b, \gamma_m, \omega) = 0 \end{aligned} \quad (41)$$

where $n, m = \dots, -2, -1, 0, 1, 2, \dots$,

Now, the simultaneous solutions of infinite order systems (36) and (41) are characterization of the problem. The equations may be truncated into square-matrix form by setting $(n = -N, \dots, -2, -1, 0, 1, 2, \dots, N)$ in (36) and using $(k = -N, \dots, -2, -1, 0, 1, 2, \dots, N)$ in (39) in conjunction with (41), to obtain

$$S_m p_m = 0 \quad (42)$$

where $m = \dots, -2, -1, 0, 1, 2, \dots$, S_m is a square matrix of order $8(2N + 1)$ that contains extremely complicated frequency dependent parameters which multiply the modal vector p_m given by

$$\begin{aligned} p_m &= [a_{-Nm}^{[1]}, b_{-Nm}^{[1]}, a_{-Nm}^{[2]}, b_{-Nm}^{[2]}, c_{-Nm}, d_{-Nm}, e_{-Nm}, f_{-Nm} \\ &\dots; a_{0m}^{[1]}, b_{0m}^{[1]}, a_{0m}^{[2]}, b_{0m}^{[2]}, c_{0m}, d_{0m}, e_{0m}, f_{0m}; \\ &\dots; a_{Nm}^{[1]}, b_{Nm}^{[1]}, a_{Nm}^{[2]}, b_{Nm}^{[2]}, c_{Nm}, d_{Nm}, e_{Nm}, f_{Nm}] \end{aligned} \quad (43)$$

The requirement of non-trivial solution of (42) leads to frequency equation

$$|S_m| = 0 \quad (44)$$

9. Numerical Results and Discussion: For the purpose of numerical computation, we have considered magnesium material the physical data of which is given below [14]

$$\rho = 1.74 \times 10^3 \text{ Kgm}^{-3}, \quad \lambda = 2.17 \times 10^{10} \text{ Nm}^{-2},$$

$$\mu = 1.639 \times 10^{10} \text{ Nm}^{-2}, \quad T_0 = 25^\circ \text{C}$$

$$C_e = 1.04 \times 10^3 \text{ JKg}^{-1} \text{ deg}^{-1},$$

$$K = 1.7 \times 10^2 \text{ Wm}^{-1} \text{ deg}^{-1},$$

$$\beta = 2.68 \times 10^6 \text{ Nm}^{-2} \text{ deg}^{-1}$$

Due to presence of dissipation term in heat conduction equation, the frequency equation (44) in general complex transcendental equation provides us complex value of frequency (ω). The dimensionless natural frequency (Ω) are defined as $\Omega = (\omega_R b)/c_1$

where $\omega_R = \text{Re}(\omega)$.

The numerical computation has been carried out with the help of MATLAB files of the system (42) to calculate the natural frequency to determine the Fourier coefficients as a function of dimensionless eccentricity parameter. The fixed point iteration numerical technique as outlined in Sharma [15] has been used to find the roots of the secular equation (44) for all eccentricities. The computation has been performed with a truncation constant $k_{\max} = N = 20$. The variations of computer simulated natural frequency $\Omega = (\omega_R b)/c_1$ have been plotted with respect to eccentric parameter for selected inner outer radius ratios and length to radius ratios ($a/b = 0.2, 0.5, 0.9$; $L/b = 1, 2$) in figs.2 and 3. The associated circumferential/flexure mode number (n, m) is also specified in each plot.

Fig.2 displays the variation of dimensionless natural frequency $\Omega = (\omega_R b)/c_1$ for each considered circumferential/flexure mode (n, m) with eccentric parameter \bar{e} , for inner outer ratio and length to radius ratio ($a/b = 0.2, 0.5, 0.9$; $L/b = 1$). It is observed that the magnitude of dimensionless natural frequency for inner outer ratio ($a/b = 0.2$) and circumferential/flexure mode (n, m) = (0,1) increases monotonically with increasing the value of eccentricity parameter. The trends of variations of magnitude of dimensionless natural frequency for inner outer ratio ($a/b = 0.2$) and circumferential/flexure mode (n, m) = (1,1), (2,1) are almost steady for ($0 \leq \bar{e} \leq 50$) and decreases monotonically for ($\bar{e} > 50$). From fig. 2, It is revealed that the magnitude of dimensionless natural

frequency for inner outer ratio ($a/b = 0.2$) and circumferential/flexure mode (n, m) = (3,1) decreases monotonically with increasing the value of eccentric parameter in the range ($0 \leq \bar{e} \leq 65$) and increases monotonically with increasing the value of eccentric parameter for ($\bar{e} > 65$). It is also observed that the magnitude of dimensionless natural frequency for inner outer ratio ($a/b = 0.5$) and circumferential/flexure mode (n, m) = (0,1) increases monotonically with increasing the value of eccentricity parameter. The trends of variations of magnitude of dimensionless natural frequency for inner outer ratio ($a/b = 0.5$) and circumferential/flexure mode (n, m) = (1,1) are almost steady and uniform for ($0 \leq \bar{e} \leq 20$) and increase monotonically with increasing the value of eccentricity parameter for ($\bar{e} > 20$). It is also revealed that the magnitude of dimensionless natural frequency for inner outer ratio ($a/b = 0.5$) and circumferential/flexure mode (n, m) = (2,1) is almost steady and uniform for ($0 \leq \bar{e} \leq 40$) and decreases monotonically with increasing the value of eccentricity parameter for ($\bar{e} > 40$). Moreover the magnitude of dimensionless natural frequency for inner outer ratio ($a/b = 0.5$) and circumferential/flexure mode (n, m) = (3,1) decreases monotonically with increasing the value of eccentricity parameter. Fig.2 displays that the magnitude of dimensionless natural frequency for inner outer ratio ($a/b = 0.9$) and circumferential/flexure mode (n, m) = (0,1) is almost steady and uniform for ($0 \leq \bar{e} \leq 70$) and decreases monotonically with increasing the value of eccentricity parameter for ($\bar{e} > 70$). The trends of variations of magnitude of dimensionless natural frequency for inner outer ratio ($a/b = 0.9$) and circumferential/flexure mode (n, m) = (1,1) are almost steady and uniform. It is observed that the magnitude of dimensionless natural frequency for inner outer ratio ($a/b = 0.9$) and circumferential/flexure mode (n, m) = (2,1) is almost steady and uniform for

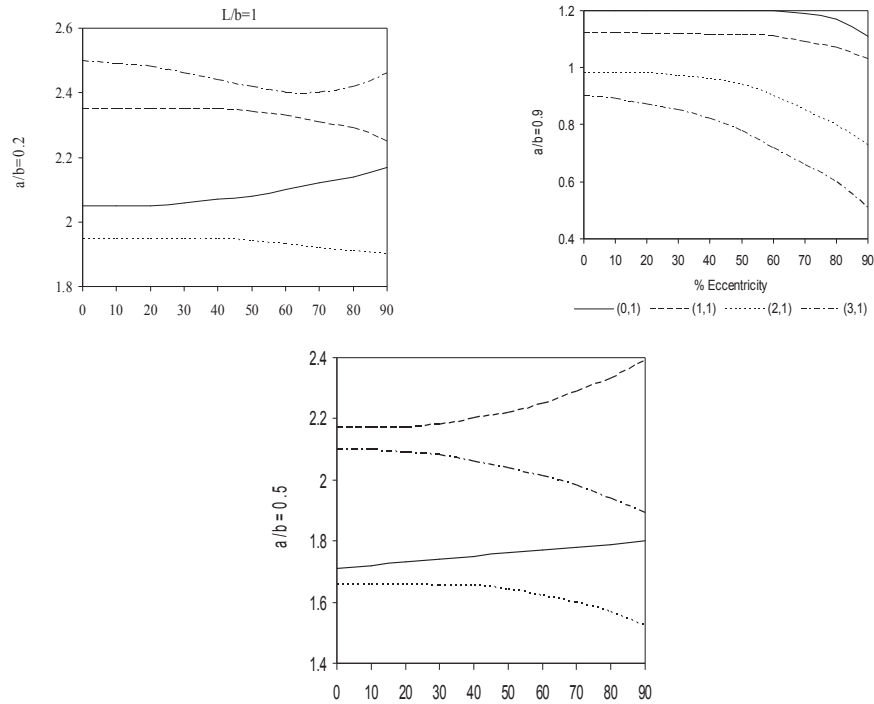


Fig.2. Variations of first several dimensionless natural frequencies ($\Omega = (\omega_R b)/c_1$) with eccentric parameter for selected inner-outer radius ratios and length to radius ratios ($a/b = 0.2, 0.5, 0.9; L/b = 1$) of finite cylinder.

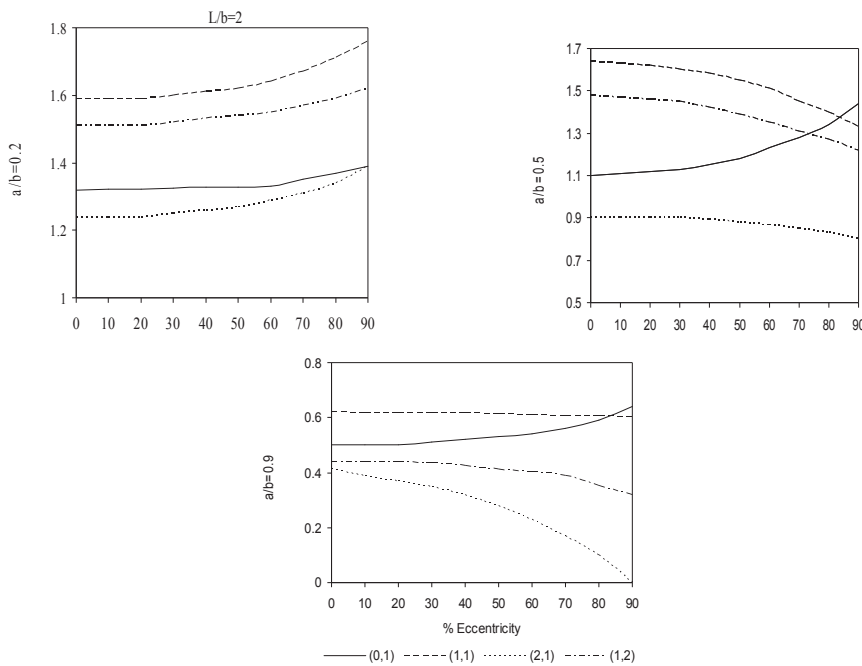


Fig.3. Variations of first several dimensionless natural frequencies ($\Omega = (\omega_R b)/c_1$) with eccentric parameter for selected inner-outer radius ratios and length to radius ratios ($a/b = 0.2, 0.5, 0.9; L/b = 2$) of finite cylinder.

($0 \leq \bar{e} \leq 30$) and decreases monotonically with increasing the value of eccentricity parameter for ($\bar{e} > 30$). For inner outer ratio ($a/b = 0.9$) and circumferential/flexure mode $(n, m) = (3, 1)$ the

magnitude of dimensionless natural frequency decreases monotonically with increasing the value of eccentricity parameter.

Fig.3 represents the variation of first dimensionless natural frequency $\Omega = (\omega_R b)/c_1$, for each considered circumferential/flexure mode (n, m) with eccentric parameter \bar{e} , for inner outer ratio and length to radius ratio $(a/b = 0.2, 0.5, 0.9; L/b = 2)$. It is observed that the trends of variations of magnitude of dimensionless natural frequency for inner outer ratio $(a/b = 0.2)$ and circumferential/flexure mode $(n, m) = (0,1), (1,1), (2,1), (1,2)$ are almost steady and uniform for all the value of eccentricity parameter. It is also observed that the magnitude of dimensionless natural frequency for inner outer ratio $(a/b = 0.5)$ and circumferential/flexure mode $(n, m) = (0,1)$ increases monotonically with increasing the value of eccentricity parameter. The trends of variations of magnitude of dimensionless natural frequency for inner outer ratio $(a/b = 0.5)$ and circumferential/flexure mode $(n, m) = (1,1), (1,2)$ are almost steady and uniform. It is also observed that the magnitude of dimensionless natural frequency for inner outer ratio $(a/b = 0.5)$ and circumferential/flexure mode $(n, m) = (2,1)$ decreases monotonically with increasing the value of eccentricity parameter. Fig.3 reveals that the trends of variations of magnitude of dimensionless natural frequency for inner outer ratio $(a/b = 0.9)$ and circumferential/flexure mode $(n, m) = (0,1), (1,1), (1,2)$ are almost steady and uniform for all the value of eccentricity parameter. It is also observed that the magnitude of dimensionless natural frequency for inner outer ratio $(a/b = 0.9)$ and circumferential/flexure mode $(n, m) = (2,1)$ decreases monotonically with increasing the value of eccentricity parameter.

Conclusions: The translation addition theorem for cylindrical wave function in conjunction with orthogonal series expansion have been employed to study the vibrations of the homogeneous, isotropic simply supported circular hollow cylinder with an inner circular cavity based on linear coupled three-dimensional thermoelasticity. The eccentric parameter enforces characteristically different effects on natural frequency, depending upon mode type, inner-outer radius ratio and length to radius ratio.

Appendix:

$$P_{1n}^{[1]}(r_j, \gamma_m, \omega) = m_1 J'_n(m_1 r_j),$$

$$P_{2n}^{[1]}(r_j, \gamma_m, \omega) = m_2 J'_n(m_2 r_j),$$

$$P_{3n}^{[1]}(r_j, \gamma_m, \omega) = \frac{in}{r_j} J_n(\alpha r_j)$$

$$P_{5n}^{[1]}(r_j, \gamma_m, \omega) = \frac{in}{r_j} J_n(m_1 r_j),$$

$$P_{6n}^{[1]}(r_j, \gamma_m, \omega) = \frac{in}{r_j} J_n(m_2 r_j),$$

$$P_{7n}^{[1]}(r_j, \gamma_m, \omega) = -\alpha J_n(\alpha r_j)$$

$$P_{8n}^{[1]}(r_j, \gamma_m, \omega) = -\frac{in\gamma_m}{r_j} J_n(\alpha r_j),$$

$$P_{9n}^{[1]}(r_j, \gamma_m, \omega) = \gamma_m J_n(m_1 r_j),$$

$$P_{10n}^{[1]}(r_j, \gamma_m, \omega) = \gamma_m J_n(m_2 r_j) \quad P_{11n}^{[1]}(r_j, \gamma_m, \omega) = 0,$$

$$P_{12n}^{[1]}(r_j, \gamma_m, \omega) = \alpha^2 J_n(\beta r_j)$$

$$Q_{1n}^{[1]}(r_j, \gamma_m, \omega) = \delta^2 m_1^2 J_n''(m_1 r_j) + (\omega^2 \delta^2 - \omega^2 - \delta^2 L_1) J_n(m_1 r_j)$$

$$Q_{2n}^{[1]}(r_j, \gamma_m, \omega) = \delta^2 m_2^2 J_n''(m_2 r_j) + (\omega^2 \delta^2 - \omega^2 - \delta^2 L_2) J_n(m_2 r_j)$$

$$Q_{3n}^{[1]}(r_j, \gamma_m, \omega) = \frac{in\delta^2}{r_j} \left[\alpha J_n'(\alpha r_j) - \frac{J_n(\alpha r_j)}{r_j} \right]$$

$$Q_{4n}^{[1]}(r_j, \gamma_m, \omega) = -\gamma_m \alpha^2 \delta^2 J_n''(\alpha r_j)$$

$$Q_{5n}^{[1]}(r_j, \gamma_m, \omega) = \frac{2in\delta^2}{r_j} \left[m_1 J_n'(m_1 r_j) - \frac{J_n(m_1 r_j)}{r_j} \right]$$

$$Q_{6n}^{[1]}(r_j, \gamma_m, \omega) = \frac{2in\delta^2}{r_j} \left[m_2 J_n'(m_2 r_j) - \frac{J_n(m_2 r_j)}{r_j} \right]$$

$$Q_{7n}^{[1]}(r_j, \gamma_m, \omega) = -\alpha^2 \delta^2 [2J_n''(\alpha r_j) + \alpha^2 J_n(\alpha r_j)]$$

$$Q_{8n}^{[1]}(r_j, \gamma_m, \omega) = \frac{2in\gamma_m\delta^2}{r_j} \left[-\alpha J_n'(\alpha r_j) + \frac{J_n(\alpha r_j)}{r_j} \right]$$

$$Q_{9n}^{[1]}(r_j, \gamma_m, \omega) = 2\gamma_m m_1 \delta^2 J_n'(m_1 r_j)$$

$$Q_{10n}^{[1]}(r_j, \gamma_m, \omega) = 2\gamma_m m_2 \delta^2 J_n'(m_2 r_j)$$

$$Q_{11n}^{[1]}(r_j, \gamma_m, \omega) = \frac{in\gamma_m\delta^2}{r_j} J_n(\alpha r_j)$$

$$Q_{12n}^{[1]}(r_j, \gamma_m, \omega) = \alpha (\omega^2 - 2\gamma_m^2 \delta^2) J_n'(\alpha r_j)$$

$$Q_{13n}^{[1]}(r_j, \gamma_m, \omega) = L_1 m_1 J_n'(m_1 r_j)$$

$$Q_{14n}^{[1]}(r_j, \gamma_m, \omega) = L_2 m_2 J_n'(m_2 r_j)$$

$$Q_{15n}^{[1]}(r_j, \gamma_m, \omega) = 0 \quad Q_{16n}^{[1]}(r_j, \gamma_m, \omega) = 0$$

where $j = 1, 2$

References:

1. J.R. Hutchinson, and S.A. El-Azhari, Vibrations of free hollow circular cylinder, *J. Appl. Mech.*, vol. 53, pp 641-647, 1986.
2. K.P. Soldatos, and V.P. Hadhgeorgian, "Three dimensional solution of the free vibration problem of homogeneous isotropic cylindrical shells and panels", *J. Sound Vib.*, vol. 137, pp. 369-384, 1990.
3. M.R. Mofakhami, H.H. Toudeshky, and Sh. H. Hashemi, "Finite cylinder with vibrations with different end boundary conditions", *J. Sound Vib.*, vol. 297, pp. 293-314, 2006.
4. I. J. Mirsky, "Wave propagation in transversely isotropic circular cylinder", *J. Acoust. Soc. Am.*, vol. 37 (6), pp. 1016-1026, 1965.
5. P.A. Martin, and J.R. Berger, "Waves in wood: free vibrations of wooden pole", *J. Mech. Phys. Solids*, vol. 49, pp. 1155-1178, 2001.
6. J.N. Sharma, "Three-dimensional vibration analysis of a homogeneous transversely isotropic cylindrical panel", *J. Acoust. Soc. Am.*, vol. 110, pp. 254-259, 2001.
7. J.N. Sharma, and P.K. Sharma, "Free vibration analysis of homogeneous transversely isotropic thermoelastic cylindrical panel", *J. Thermal stres.*, vol. 25, pp. 169-182, 2002.
8. H.B. Khurasia, and S. Rewtant, "Vibration analysis of circular plate with hole", *J. Appl. Mech.*, vol. 45, pp 215-217, 1978.
9. P.A.A. Laura, C.P. Filipitch, R.E. Rossi, and J.A. Reyes, "Vibrations of rings of variable cross section", *J. Appl. Acoust.*, vol. 25, pp. 225-234, 1988.
10. H. Zhong, and T. Yu, "Flexural vibration analysis of an eccentric annular Mindlin plate", *Arch. Appl. Mech.*, vol. 77, pp. 185-195, 2007.
11. M. Seyyed Hasheminejad, and Y. Mirzaei, "Free vibration analysis of an eccentric hollow cylinder using exact 3D", *J. Sound Vib.*, vol. 326, pp. 687-702, 2009.
12. Y.H. Pao, and C.C Mow, "Diffraction of Elastic wave and Stress Wave Concentration", Crane Russak, New York, 1994.
13. Ye. A. Ivanov, "Diffraction of Electromagnetic Waves on Two Bodies", Nauka I Tekhnika, 1968.
14. P.K. Sharma, D. Kaur, and J.N. Sharma, "Three-dimensional vibration analysis of thermoelastic cylindrical panel with voids", *Int. J. Solids. Struct.*, vol. 45, pp. 5049-5058, 2008.
15. J. N. Sharma, "Numerical Methods for Engineers and Scientists", Narosa Publishing House New Delhi, India, 2008.

* * *

Department of Mathematics, Lyallpur Khalsa College, Jalandhar-144001